Journal of Cleaner Production 288 (2021) 125564

Contents lists available at ScienceDirect

Journal of Cleaner Production

journal homepage: www.elsevier.com/locate/jclepro

A multi-objective optimization model for fast electric vehicle charging stations with wind, PV power and energy storage

Baojun Sun

College of Computer and Information Management, Inner Mongolia University of Finance and Economics, Hohhot, China

ARTICLE INFO

Article history:
Received 9 September 2020
Received in revised form
10 December 2020
Accepted 14 December 2020
Available online 16 December 2020

Handling editor: Kathleen Aviso

Keywords:
Multi-objective optimization
Fast electric vehicle charging station
Energy storage
Wind power
Photovoltaic power
Optimal design

ABSTRACT

The construction of fast electric vehicle (EV) charging stations is critical for the development of EV industry. The integration of renewable energy into the EV charging stations comprises both threats and chances. A successful and reasonable capacity configuration and scheduling strategy is beneficial and significant. This paper studies the optimal design for fast EV charging stations with wind, PV power and energy storage system (FEVCS-WPE), which determines the capacity configuration of components and the power scheduling strategy. Firstly, an EV charging load simulation model considering demand response is built, which dynamically modified charging expectation under time-of-use electricity price. Secondly, based on the system design, a multi-objective optimization model is proposed with minimum objectives of cost of electricity and pollution emissions. Then, this model is solved by a hybrid optimization algorithm which combines multi-objective particle swarm optimization (MOPSO) algorithm and Technique for Order Preference by Similarity to Ideal Solution (TOPSIS) method. Finally, the proposed optimization framework is applied to a case in Inner Mongolia, China. A scenario analysis is conducted and concludes that the renewable energy supplies, the connection with utility grid and demand response can help improve the performance on optimization objectives. A sensitivity analysis is also performed to verity the model's effectiveness. In addition, the proposed method is compared with simulated annealing and genetic algorithm to show its faster computation speed and higher solution quality.

1. Introduction

In recent years, energy shortage and environmental pressure are becoming increasingly severe, and traditional fuel vehicles are causing more and more concern due to their high energy consumption and carbon emissions. Developing electric vehicles (EV) is an effective way to reduce China's dependence on oil resources and improve environmental pollution. As a result, the number of EVs is expected to grow exponentially over the next few years. At present, the EV industry is still at the stage of development and one of the important factors restricting its development is the lack of charging infrastructure (Xu et al., 2017). By November 2019, China has built 496,000 public charging piles and 678,000 private charging piles, far below expectations. Although EV drivers can charge their cars at home, the long charging time still affects the efficiency of use. In order to promote the development of EV industry, the construction of fast EV charging stations is essential. Compared with slow charging, fast charging has the disadvantage of large power demand and great impact on the national power grid. In order to solve this problem, wind power, photovoltaic (PV) power generation and energy storage systems are applied in fast charging stations to provide convenient and safe charging service for EVs (Zhang and Han, 2017).

The application of wind, PV power generation and energy storage system (ESS) to fast EV charging stations can not only reduce costs and environmental pollution, but also reduce the impact on utility grid and achieve the balance of power supply and demand (Esfandyari et al., 2019). It is of great significance for the construction of fast EV charging stations with wind, PV power and ESS (FEVCS-WPE) to predict the load demand of EVs and determine the capacity configuration of system components (Dominguez-Navarro et al., 2019). Too much capacity will give rise to the waste of costs and resources. While low capacity cannot meet the load demand and a large amount of electricity should be needed from the national power grid, which will aggravate the impact on utility grid. At present, many scholars have carried out researches on capacity configuration of EV charging stations. According to the

E-mail address: sunbj@imufe.edu.cn.

https://doi.org/10.1016/j.jclepro.2020.125564
0959-6526/

existing research, the main factors affecting capacity configuration are the load in the system, the optimization objective and the optimization method. Therefore, taking these three factors into consideration, this paper tries to propose a more accurate capacity configuration and power scheduling method. Firstly, this paper builds an EV charging load simulation model considering price-based demand response (DR). On the basis of the load demand result, a bi-objective optimization model is constructed to investigate the optimal capacity configuration of FEVCS-WPE and the optimal power dispatch strategy. Besides, the proposed optimization model is solved by multi-objective particle swarm optimization (MOPSO) algorithm and the final optimum is selected by Technique for Order Preference by Similarity to an Ideal Solution (TOPSIS) method. Finally, a case study in China is conducted.

The contributions of this paper are summarized as follows:

(1) The energy source of the existing fast EV charging stations is basically the power grid. The research on hybrid energy system considering renewable energies and energy storage is lacking. Therefore, this paper proposes a fast EV charging station design with wind, PV power generation and ESS, connected with utility grid.
(2) In the FEVCS-WPE system, most research on capacity configuration regards the load of EVs as fixed, while few literatures consider the DR of EVs. Therefore, this paper builds an EV charging load simulation model by dynamically adjusting the EV charging expectations according to time-of-use (TOU) electricity price.
(3) With objectives of minimizing the COE and pollution emissions, an optimization design model for FEVCS-WPE is proposed. The optimal capacity of system components and the optimal power scheduling strategy is determined.
(4) To the best knowledge of authors, there is no literature to combine MOPSO and TOPSIS to configure the size of FEVCS-WPE. Therefore, in this paper, a hybrid optimization algorithm combining MOPSO and TOPSIS method is employed, in which MOPSO obtains the Pareto solutions and TOPSIS selects the optimal one.

The rest of this study is organized as follows. Section 2 reviews the existing research on EV charging power, capacity configuration and optimization algorithms. Section 3 simulates EV power load considering price-based DR. Section 4 proposes models of FEVCS-WPE components. Based on the EV power load and component models, Section 5 builds a bi-objective optimization framework to design the optimal size and scheduling for FEVCS-WPE. In Section 6, a case in China is studied and discussed.

2. Literature review

2.1. EV charging power simulation and prediction

In the proposed optimization problem in this study, predicting the EV charging load is the basis for constructing the whole system. At present, a large number of scholars have carried out relevant research on EV charging load prediction and achieved remarkable results. The research methods can be divided into four categories: constant method, behavioral analysis method, simulation method and statistical analysis method. (1) Constant method is to set the charging load of EVs directly as a constant to simplify the simulation process. Vermaak and Kusakana (2014) studied the charging strategies of different charging stations in the rural areas of the Democratic Republic of Congo, on the premise that the charging load of charging stations is constant. Hafez and Bhattacharya (2020) designed the EV charging stations and set the charging load as a constant with the objectives of life cycle cost and emissions. Fathabadi (2017) also directly set the charging load as a constant. This method reduces the difficulty of designing and optimizing EV charging stations. However, the determination of EV charging load is a very complex problem, and there are many influencing factors, such as the type of EV, battery capacity, power of charging piles and charging mode, etc. The average value or constant method may affect the design of charging stations. (2) Behavioral analysis means to build a model reflecting the travel rules of EV users in a certain area and within a certain period of time, so as to calculate the charging load. In behavioral analysis, travel chain, Markov chain and traffic travel matrix are usually used to simulate the real situation or the proposed assumptions. Yi et al. (2020) estimated the relationship between EV charging station layout and charging probability based on GPS survey data of three cities and calculated the charging probability of travel chain by using heuristic algorithm. Zhang et al. (2014) used Markov chain to determine the transfer probability of EV travel destination, and based on the analysis results, proposed a double-layer charging load prediction model based on Monte Carlo (MC) simulation. In addition, Pan et al. (2018) conducted charging load analysis based on the travel behavior patterns of EV users. (3) Simulation method is a method to deal with the randomness of EV charging behavior. MC simulation and random simulation based on queuing theory are commonly applied. Baharin and Abdullah (2013), by analyzing the time distribution of the last return of EVs in each day, used MC to randomly simulate the initial charging time of EVs and conduct charging load simulation. Chang et al. (2019) analyzed the travel pattern of EV users and selected three factors influencing EV charging: initial state-of-charge (SOC), starting time, and EV battery charging characteristics, and then used MC to simulate the load. Bae and Kwasinski (2012) calculated the charging load of EVs at roadside charging stations on the basis of the statistics of vehicles entering and leaving the expressway section through queuing theory. Zhang et al. (2015) analyzed the actual survey data of electric taxis, used M/C/G queuing model to analyze the influence of SOC characteristics of electric taxis on queuing system, and proposed relevant improvement measures. (4) Statistical analysis is a method to analyze historical data and make a prediction by using big data, artificial intelligence, cloud computing and other high-tech information technologies on the basis of traditional mathematical statistical analysis and probability theory analysis. Lee et al. (2012) used probability estimation and cluster analysis to analyze the distribution of charging load. Li et al. (2019) used the k-Nearest Neighbors algorithm in machine learning to simulate the random characteristics of users' travel behaviors and predict the charging load of EV charging stations.

Among these four calculation methods, the constant method is less used due to inaccuracy of the results. Behavioral analysis and simulation method have stronger applicability and less dependence on historical data, but the analysis process is more complex, and the reliability of analysis results are not as good as statistical analysis. Therefore, these three methods should be applied comprehensively to complement each other.

2.2. Capacity configuration optimization

Capacity configuration optimization is critical for a newly built EV charging station, and the choice of optimization objectives also has a great impact on the result of capacity configuration. At present, the research of capacity configuration optimization can be divided into single-objective and multi-objective optimization.

(1) Single-objective optimization. In the existing research on single-objective optimization problems, the objectives are

basically related to cost indicators, such as the cost of electricity (COE) (Javed et al., 2019), net present cost (NPC) (Das et al., 2019) and life cycle cost (LCC) (Zhang et al., 2019). Ekren and Ekren (2010) studied a PV/wind hybrid energy conversion system on a campus in Turkey and optimized the system capacity using simulated annealing (SA) algorithm with the objective of minimum of total cost. Through comparative analysis, it showed that this method was obviously superior to mathematical optimization method. Dai et al. (2019) studied the capacity configuration of PV/EV charging stations with the goal of minimizing the cost. Amrollahi and Bathaee (2017) studied an independent microgrid and optimized the capacity of wind, PV and ESS by minimizing the total net present cost. Kerdphol et al. (2016) studied the capacity optimization of the battery ESS in an independent microgrid by minimizing the total energy storage cost. Zhang et al. (2019) studied the wind/PV/hydrogen storage energy system with minimizing the total LCC. Liu et al. (2018) used PSO algorithm and considered LCC as the objective function to propose the capacity optimization method of microgrids. Ma et al. (2014) studied the PV/wind/ESS system capacity configuration based on NPC and COE, but they were both cost indicators. Different from the above literature, Acuna et al. (2017) suggested that the hybrid wind/PV system is an effective solution to alleviate the growing energy pressure, but because of the strong randomness and volatility of renewable energy, the reliability analysis must be carried out. Therefore, a reliability indicator called maxENS was proposed to measure the degree of reliability using a probabilistic approach.

(2) Multi-objective optimization. Single-objective optimization only considers one aspect of the impact and has certain limitations, usually ignoring the role of the environment, reliability and other aspects (Mazzeo et al., 2020a). Therefore, many scholars combined economic indicators, environmental benefit indicators and reliability indicators to study capacity allocation (Mazzeo et al., 2020b). Shakerighadi et al. (2018) suggested to consider financial and technical aspects together in order to operate the system optimally and securely. Yang et al. (2009) believed that most of the optimization problems related to the hybrid energy system only considered the cost minimization and ignored the overall design characteristics of the system, which led to inaccurate optimization results. Therefore, they used the power failure rate and annual cost of the system as objective functions, and employed genetic algorithm to conduct simulation research. Xu et al. (2018) applied wind power and hybrid ESS to the EV charging stations and optimized the capacity of ESSs considering the maximum of annual profit and the minimum of wind curtailment. Das et al. (2020) considered battery degradation, energy cost, CO_2 emission and grid net exchange as objectives, and used augmented non-dominated constraint method (ANEC) and AHP method to optimize the charging and discharging strategies for EVs. Moghaddam et al. (2011) considered operating cost minimization and pollutants emission minimization as objective functions and applied adaptive modified particle swarm optimization algorithm. In their further research, the fuzzy self-adaptive particle swarm optimization algorithm is proposed to optimize the operation management of microgrids (Moghaddam et al., 2012). Ramli et al. (2018) studied the capacity optimization of a microgrid system with PV, wind and diesel considering loss of power supply probability (LPSP) and COE as the objective functions. Tito et al. (2016) combined exhaustive search method and genetic algorithm (GA) to size an off-grid system with wind, PV and batteries considering unmet load and cost. Eriksson and Gray (2019) considered levelized cost of electricity, socio-political index, LPSP and carbon footprint of electricity as optimization objectives, and obtained the optimal system capacity by using a weighted constrained multi-objective optimization algorithm (NWCMO). In addition, Xu et al. (2020) studied capacity configuration by taking cost of electricity, LPSP and other indicators as optimization objective functions. Wang et al. (2017) employed NSGA-II to optimize the size of a typical stand-alone hybrid renewable energy system with the objectives of minimizing cost, LPSP and greenhouse gas emission. The summary of the above research is presented in Table 1.

The objective functions are generally determined from three aspects: economy, reliability and environmental benefits. Economic indicators include COE and NPC while reliability indicators generally consider LPSP. This paper studies the design of FEVCS-WPE, which is also connected to the utility grid, so this system will not be short of electric power. Therefore, in this paper, optimization objectives are selected mainly from two aspects of the economic and environmental benefits. Besides, this paper not only determines the capacity configuration, but also investigates the optimal charging/discharging pattern for ESS.

2.3. Optimization algorithms

The problem of energy management and capacity configuration in power system is well known as an optimization problem. When there are two or more objective functions in the problem, the calculation difficulty will increase. A widely-used method to solve the multi-objective optimization models is to assign weight to each objective and convert it into a single-objective function, which requires a lot of calculation (Naidu et al., 2014). Moreover, in the multi-objective optimization, each objective is not independent and there may be some conflicts between them, so that multiple objectives cannot be met at the same time and compromises need to be made. As a result, the weighted sum method has certain one-sidedness (Shakerighadi et al., 2018). Besides, multi-objective optimization problems can be solved by different methods, such as (1) probabilistic approach (Fazlalipour et al., 2018), (2) analytical methods (Mercier et al., 2009), (3) mathematical optimization including integer linear programming (Montoya et al., 2020) and dynamic programming (Nguyen et al., 2015), etc., (4) multi-objective evolutionary algorithms (MOEA) (Gomez-Gonzalez et al., 2020).

Compared with MOEA, probability methods use statistical technology to change the value of the decision variables to obtain the optimization result, which requires a large amount of calculation and a large number of iterations to achieve a high-precision result (Esmaeili et al., 2019). Analytical methods cannot be applied to highly nonlinear problems or problems with more than 2 or 3 independent parameters. Additionally, mathematical optimization is more suitable for small-scale problems because of its computation complexity and is not practical in engineering problems. The study shows that MOEA is an effective approach for the multi-objective optimization of capacity optimization and energy management (Bukar and Tan, 2019).

The biggest advantage of the multi-objective optimization algorithms is that different feasible solutions can be obtained in a single run (Xu et al., 2018). In MOEAs, genetic algorithm (GA) (Liu et al., 2019), SA (Ekren and Ekren, 2010) and PSO (Li et al., 2020) are widely used intelligent algorithms. GA is usually used to deal with the optimization problem of a hybrid system with a lot of

Table 1
Summary of research on capacity configuration optimization.

References	Components	Objectives	Method
Ekren and Ekren (2010)	PV, Wind, battery banks	Total cost	SA
Dai et al. (2019)	PV, BESS, grid	COE	Multi-agent PSO
Amrollahi and Bathaee (2017)	PV, wind, BESS	NPC	Mixed integer linear programming
Singh et al. (2017)	Wind, PV, diesel, BESS	COE, NPC	GA
Kerdphol et al., 2016a	BESS	total BESS cost	PSO-based frequency control
Javed et al. (2019)	PV, Wind, BESS	COE	GA
Amrollahi and Bathaee (2017)	PV, pumped storage, BESS, biogas	NPC	Water cycle algorithm
Zhang et al. (2019)	Wind, PV, hydrogen, BESS	LCC	Harmony search, chaotic search, and SA
Liu et al. (2018)	PV/Wind/CHP/BESS	LCC	PSO
Acuna et al. (2017)	PV, Wind	maxENS	Probability distributions
Yang et al. (2009)	PV, Wind, battery banks	LPSP, annualized cost	GA
Xu et al. (2018)	Wind, batteries, supercapacitors	Wind curtailment rate and annual profit	NSGA-II and VIKOR
Das et al. (2020)	PV, BESS, grid	Wind curtailment rate and annual profit	ANEC-AHP
Moghaddam et al. (2011)	micro-turbine, fuel cell, PV, Wind, battery	Operating cost Pollutants emission	Adaptive modified particle swarm optimization algorithm
Moghaddam et al. (2012)	micro-turbine, fuel cell, PV, Wind, battery	Operating cost Pollutants emission	Fuzzy self adaptive particle swarm optimization
Ramli et al., 2018a	PV, wind, diesel	COE, LPSP	Self-adaptive differential evolution algorithm
Tito et al. (2016)	PV, wind, diesel	Unmet load cost	Exhaustive search method and GA
Eriksson and Gray (2019)	PV, wind, BESS	LCOE, LPSP,	NWCMO
Xu et al. (2020)	PV, wind, pump storage, hydropower,	COE, LPSP	MOPSO
Wang et al. (2017)	Wind, PV, diesel, BESS	Cost, LPSP	NSGA-II

parameters and can be evaluated according to the fitness function. However, it is difficult to encode in this algorithm (Zhang et al., 2020). Ren et al. (2019) designed a distributed energy system and used NSGA-II to determine the optimal operation and scheduling strategy. SA algorithm can be used in non-deterministic problems (Ekren and Ekren, 2010). Zhang et al. (2019) evaluated the reliability of a hybrid renewable energy system with the minimum life cycle cost, by using SA. PSO is an optimization algorithm based on swarm intelligence theory, which is generated by cooperation and competition among particles in a swarm. Shang et al. (2016) optimized the ESS capacity in a stand-alone renewable energy system based on PSO. Hakimi and Moghaddas-Tafreshi (2009) employed PSO to study the capacity of components in a stand-alone hybrid energy management system in Iran and it was proved that this method was effective. In summary, compared with PSO, GA and SA have some weaknesses. In GA, the coding is complex, and the search speed is slow. The selection of parameters such as crossover rate and mutation rate basically depends on experience, which has a great impact on the quality of solutions. Similarly, the convergence speed of SA is also slow, and the selection of parameters has a great influence on the result. PSO is an efficient parallel search algorithm, which is suitable for optimization in a dynamic and multi-objective optimization environment. It is easy in coding and has strong robustness for control parameter, faster computing speed and better global search capability (Sun et al., 2017).

Multi-objective optimization will produce a group of non-dominated solutions to form the Pareto front, but how to determine the optimal solution from these solutions is a big problem for decision makers. Therefore, some literatures introduced multi-attribute decision-making (MADM) approaches to sort all feasible Pareto solutions to obtain the optimal one. Xu et al. (2018) obtained the Pareto solutions by NSGA-II and determined the optimum by VIKOR method. Sarshar et al. (2017) used TOPSIS method to choose the optimal solution from the Pareto solution set solved by NSGA-II. Yousefi et al. (2017) combined GA and AHP method to investigate the optimal configuration of a hybrid combined cooling heat and power system. Nguyen et al. (2020) combined an extended power-pinch analysis (EPoPA) optimization algorithm and TOPSIS method to optimize the capacity of a hybrid microgrid system.

Therefore, in this paper, a multi-objective optimization algorithm and a MADM method are applied to solve the proposed optimization problem.

As evidenced by the literature review, the main research gaps can be summarized as follows. (1) The energy source of the existing fast EV charging stations is basically the power grid. The research on hybrid energy system considering renewable energies and energy storage is lacking. (2) In the FEVCS-WPE system, most research on capacity configuration regards the load of EVs as fixed, while few literatures consider the DR of EVs. (3) For capacity configuration optimization of EV charging stations with renewable energy, few literatures considered multiple objectives such as economic and environmental benefits. Moreover, in this field, few scholars combined multi-objective optimization algorithm and MADM to select the optimal solution in order to support investors to make more accurate decisions.

Therefore, the purpose of this paper is to solve the gap in the current literature by building an optimization design model that considers DR. Firstly, taking the DR into consideration, the charging load of EVs at each moment is simulated according to a dynamic adjustment method under peak-flat-valley electricity price. Then a multi-objective optimization framework for FEVCS-WPE design is proposed considering the minimum of COE and pollutant emissions. To solve this model, MOPSO is utilized to obtain Pareto front and TOPSIS is applied to select the optimal solution from multitudinous Pareto solutions. Finally, the proposed model is applied in a case in Inner Mongolia, China. Based on the above measures, this paper can provide a more efficient capacity configuration optimization method for decision makers.

3. EV load demand simulation model considering DR

In order to predict the EV load demand, the EV charging process is simulated in this section considering price-based DR where TOU electricity price is used.

3.1. Charging duration

The prediction of EV charging load is highly correlated with the required charging time, and therefore determining accurate charging duration is the premise of charging power calculation. The initial charging time and charging duration jointly determine in which period the EV is charging. To date, since most EVs use lithium-ion batteries, the charging process mainly includes two phases: constant voltage charging and constant current charging. Since the electricity of EV charging mainly comes from the constant voltage stage and the charging power fluctuations at this stage are negligible, the whole charging process will be considered as a constant voltage charging period with a constant power. The charging duration of EVs is mainly affected by battery capacity, starting and expected SOC and charging power. The calculation of charging time is presented as Eq. (1).

$$T_{cev} = \frac{SOC_E - SOC_S}{\eta P} E \tag{1}$$

where T_{cev} is the charging duration. SOC_E is the expected SOC. SOC_S is the start SOC. P is the charging power. E is the battery capacity. η is the charging efficiency, mainly valued as 0.9.

3.2. Dynamic adjustment of EV charging expectation

3.2.1. Determination of peak, flat and valley period

The peak, flat and valley period is determined based on two principles. First, the charging infrastructure is mainly used by electric taxis and household electric cars. The charging time of electric taxis is generally during the shift and rest time of 11:00–15:00 and 02:00–06:00. The charging time of household electric cars is during the period of 18:00 to 20:00 after work. Second, the main energy sources in the system are wind and PV power. The PV system can only generate electricity when there is sunlight in the daytime.

According to the above two principles, this paper sets the peak period of this system as 02:00–06:00 and 18:00–20:00, the flat period as 06:00–18:00, and the valley time period as 00:00–02:00 and 20:00–24:00.

3.2.2. Dynamic adjustment of EV charging expectation under TOU price

In this paper, it is assumed that EV users in this system will actively respond to the TOU electricity price policy in order to minimize their own costs. Therefore, users will choose to shorten the charging time during peak hours and reduce the charging expectation SOC_E. The dynamic adjustment rules of the EV charging expectation under TOU price are as follows.

(1) If the start and end time of charging are both within peak period, the SOC_E is set as 0.8 to shorten charging time and reduce charging cost.
(2) If the start time of charging is within peak period and the end time is within valley period, the electric car charging will experience the peak to the valley. So, if the SOC of EV batteries reaches 0.8 in the peak period, then SOC_E is set as 0.8. Otherwise, the expected SOC is set as 1 and the charging duration is updated according to Eq. (1).
(3) If the start and end time of charging are both within valley period, the entire charging process of the EV will be during the valley period and SOC_E is set as 1.
(4) If the EV charging starts at valley time and ends at peak time, the electric car will experience from valley to peak. Therefore, if the SOC reaches 0.8 before peak time, then the charging process ends at the end of valley period or when the batteries are fully charged. Otherwise, SOC_E is set as 0.8 and the charging duration is updated by Eq. (1).

3.3. EV load simulation process

Considering the behavior habits of EV users, charging duration, DR and other factors, the EV charging process is simulated and the charging load is predicted. The specific steps are presented as Fig. 1.

4. Models for FEVCS-WPE components

4.1. System design

In the proposed FEVCS-WPE, the electricity is mainly provided by wind, PV power generation and energy storage system. Meanwhile, FEVCS-WPE is also connected to the utility grid, so that the power can be sold to or be purchased from the national power grid. FEVCS-WPE can not only achieve the balance between supply and demand, but also gain profits from the utility grid, which can improve the efficiency of the system. At present, FEVCS-WPE has become a typical mode of renewable energy consumption and has been applied in many cities.

The proposed FEVCS-WPE consists of wind turbines (WT), PV panels, battery energy storage system (BESS), EVs and utility grid. The entire FEVCS-WPE is controlled by the energy management control center, which realizes the generation, transmission and dynamic interaction with utility grid. The component descriptions of the FEVCS-WPE system are as follows.

(1) WT and PV panels are respectively connected to direct current (DC) bus through alternating current (AC)/DC module and DC/DC module to provide electricity for charging EVs.
(2) BESS is connected to FEVCS-WPE system through DC bus, which can not only provide electricity for EVs, but also store the excessive energy of the system to regulate electric power.
(3) EV charging devices realize the storage of electricity from WT, PV panels, BESS and utility grid into EVs, so EVs mainly exist as loads in FEVCS-WPE.
(4) Utility grid mainly provides energy backup for FEVCS-WPE. When energy from WT, PV modules and BESS cannot meet the demand of EV charging, the system will buy electricity from the utility grid under real-time electricity price to meet the balance of the supply and demand. On the contrary, when energy from WT, PV and BESS is greater than the power demand of EVs, the system will sell the excess energy to the utility grid to earn profits.

4.2. Wind turbines

The wind power output mainly depends on the characteristics of WTs and the speed at turbine hub altitude, which can be expressed by Eq. (2).

$$P_{WT}(t) = \begin{cases} 0, & (v \le v_{cut-in}) or (v \ge v_{cut-out}) \\ P_r \left(\dfrac{v(t)^3 - v_{cut-in}^3}{v_r^3 - v_{cut-in}^3} \right), & v_{cut-in} < v \le v_r \\ P_r, & v_r < v \le v_{cut-out} \end{cases} \tag{2}$$

where $P_{WT}(t)$ is the output power. P_r is the output at rated speed. $v(t), v_r, v_{cut-in}$ and $v_{cut-out}$ respectively represent the actual wind speed, rated speed, cut-in and cut-out speed for the WT at time t.

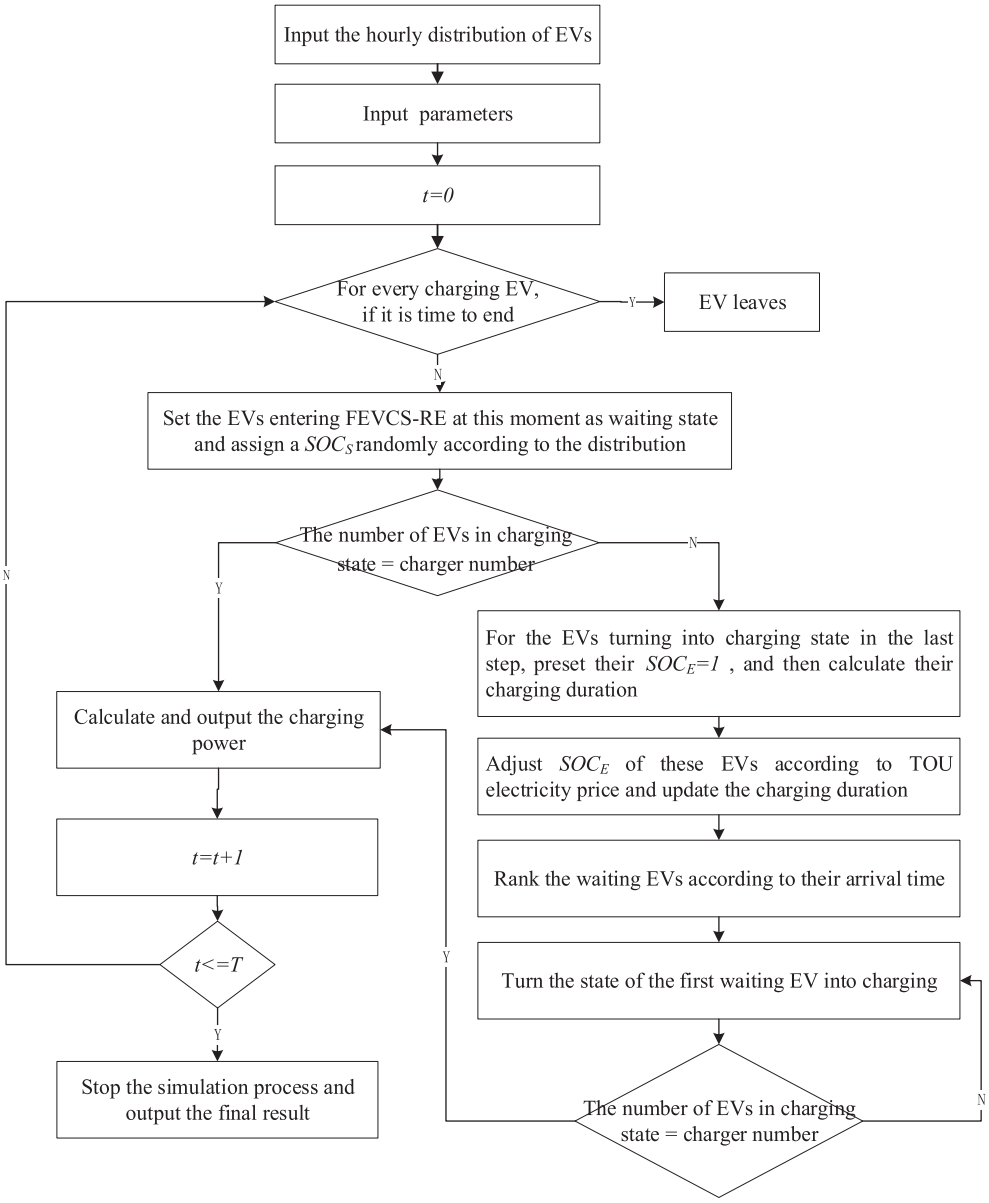

Fig. 1. The process to simulate EV charging load.

Step 1 Input the number of charging piles (assuming that all charging piles are vacant in the initial state), and calculate the number of EVs entering the charging station at each time interval based on historical data. According to the research data, the charging power and battery capacity of EVs are input into the model, and the distribution of initial SOC of EVs is simulated. t = 0.
Step 2 For the EVs in charging state, the charging duration determines whether the charging process is finished. If it is finished, this EV will leave the station.
Step 3 Set the EVs entering FEVCS-WPE at this moment as waiting state and assign a SOC_Srandomly according to the distribution. If there are no vacant charging piles, go to Step 5. If the number of vacant charging piles is more than 0, the EVs in the waiting state are turned into charging state one by one according to the order of EV arrival until all the charging piles are occupied.
Step 4 For the EVs turning into charging state in the last step, preset their SOC_E = 1, and then calculate their charging duration according to Eq (1). According to the end time of EV charging, adjust SOC_E of these EVs according to TOU electricity price and update the charging duration T_c.
Step 5 Based on the power of each charging vehicle, the power output at this moment can be calculated.
Step 6 Then t = t+1. If t reaches the end of simulation period, go to Step 7. Otherwise, go to Step 2.
Step 7 Output the charging power of each moment.

The relationship between wind speed and power output is illustrated in Fig. 2.

The speed at turbine hub $v(t)$ can be computed based on the wind turbine height h, the wind tower height h_{ref} and the wind speed at the wind tower v_{ref}, shown as Eq. (3).

$$v(t) = v_{ref} \times \left(\frac{h}{h_{ref}}\right)^{\gamma} \tag{3}$$

whereγ is friction coefficient, usually valued as 1/7.

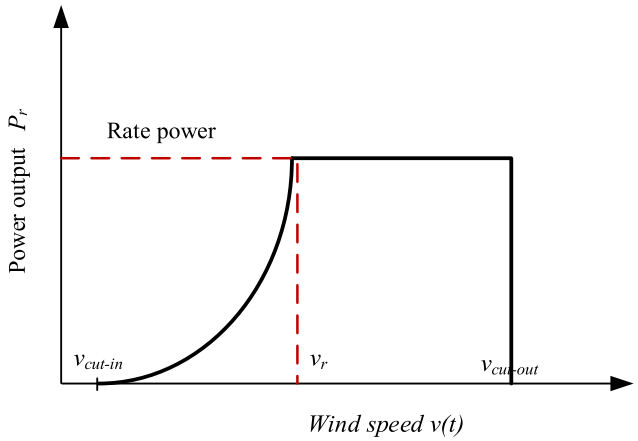

Fig. 2. Wind speed and output.

4.3. PV system

PV power generation is a process of converting solar radiation into electrical energy by using the photoelectric effect (Hernández et al., 2020). PV system is known as the most ideal new energy due to its characteristics of safety, reliability and pollution free, composed of solar panels, solar inverters, cables, other electrical accessories, etc.

The PV output is given by Eq. (4).

$$P_{PV}(t) = \frac{G_t(t)}{G_{ref}} \times P_{PV-STC} \times \eta_{PV} \times [1 - \beta_T(T_c - T_{C-STC})] \tag{4}$$

where $G_t(t)$ is the solar radiation. G_{ref} is $1000W/m^2$. η_{PV} is the generation efficiency. P_{PV-STC} is the rated power of PV panel which is given by the supplier. β_T is the temperature coefficient which ranges from 0.004 to 0.006 per $^\circ C$. T_C is the cell temperature, given by Eq. (5). T_{C-STC} is the cell reference temperature.

$$T_C = T_{amb} + (NOCT - 20) \times \frac{G_t(t)}{800} \tag{5}$$

where NOCT is normal operation cell temperature and T_{amb} is the ambient temperature.

4.4. BESS model

The charging/discharging process of BESS is shown as Eq. (6).

$$E_{BESS}(t) = E_{BESS}(T-1) \times (1-\sigma) + [P_{ch}(T) \times \eta_{ch} \times \mu_1(t) - P_{dis}(t)/\eta_{dis} \times \mu_2(t)] \times \Delta t \; t = [1, 2, \cdots, T] \tag{6}$$

where $E_{BESS}(t)$ is the electricity in BESS at time t. σ is self-discharge rate. $P_{ch}(t)$ and η_{ch} are the charging power at time t and charging efficiency respectively. $P_{dis}(t)$ and η_{dis} are the discharging power at time t and discharging efficiency respectively. Δt is the time interval. Besides, BESS needs to meet the following constraints.

$$\mu_1(t) + \mu_2(t) = [0, 1] \tag{7}$$

$$\mu_1(t) = [0, 1] \tag{8}$$

$$\mu_2(t) = [0, 1] \tag{9}$$

These constraints mean that BESS cannot be charged and discharged simultaneously at each time interval. In Eq. (7), $\mu_1(t)$ and $\mu_2(t)$ represent the charging and discharging state of BESS respectively. 1 means BESS is in charging or discharging process while 0 means the opposite.

The power of BESS and the electricity in BESS should also meet the following constraints.

$$P_{ch}(t) \le P_{BESS} \tag{10}$$

$$P_{dis}(t) \le P_{BESS} \tag{11}$$

$$E_{BESS\min} \le E_{BESS}(t) \le E_{BESS\max} \tag{12}$$

where P_{BESS} is the rated power; $E_{BESS\max}$ and $E_{BESS\min}$ are the maximum and minimum electricity allowed to be stored in BESS respectively. $E_{BESS\min}$ is given by Eq. (13).

$$E_{BESS\min} = (1 - DOD)E_{BESS\max} \tag{13}$$

where DOD is the allowable depth of discharge.

5. Framework of the optimization model

In the proposed bi-objective optimization model, the decision variables are the number of WTs, PV panels and batteries, the charging/discharging power of BESS, and the power exchanged with utility grid at each time interval. The objectives are to minimize COE and pollution emissions. Besides, MOPSO and TOPSIS are applied to solve this model. Finally, the optimal capacity and power scheduling strategy of FEVCS-WPE are determined.

5.1. Optimization objectives

5.1.1. Cost of electricity

The first objective is to minimize the COE of the FEVCS-WPE system. The COE is calculated by Eq. (14).

$$COE = \frac{NPV}{365^* \sum_{t=1}^{T} P_{Load}(t)} \times CRF \tag{14}$$

where $P_{Load}(t)$ is the EV charging load at time t. CRF is the capital recovery factor, given by Eq. (15).

$$CRF = \frac{r(1+r)^y}{(1+r)^y - 1} \tag{15}$$

where y is the system lifetime and r is the discount rate.

NPC includes the total cost of wind, PV, BESS and the cost of exchanging energy with utility grid, given by Eq. (16).

$$NPC = \sum_{k=\{Wind,PV,BESS\}} C_k \times N_k + \frac{C_{grid}}{CRF} \tag{16}$$

where N_k and C_k represent the number and the cost of the kth component. C_{grid} is the annual cost of exchanging energy with utility grid.

The costs of WT, PV panels and BESS consist of investment cost (IC) IC_k, replacement cost (RC) RC_k and operation and maintenance cost (OM) OM_k, given by Eq. (17).

$$C_k = IC_k + RC_k + OM_k \tag{17}$$

In this model, we assume that the lifetime of WT and PV system is the same as the FEVCS-WPE system. Therefore, $RC_{WT} = RC_{PV} = 0$.

The costs of each component are calculated by Eqs. 18–24.

$$IC_{WT} = AIC_{WT} \times N_{WT} \tag{18}$$

$$IC_{PV} = AIC_{PV} \times N_{PV} \tag{19}$$

$$IC_{BESS} = AIC_{BESS} \times N_{BESS} \tag{20}$$

$$OM_{WT} = AOM_{WT} \times N_{WT} \times \sum_{n=1}^{y} \left(\frac{1}{1+r}\right)^n \tag{21}$$

$$OM_{PV} = AOM_{PV} \times N_{PV} \times \sum_{n=1}^{y} \left(\frac{1}{1+r}\right)^n \tag{22}$$

$$OM_{BESS} = AOM_{BESS} \times N_{BESS} \times \sum_{n=1}^{y} \left(\frac{1}{1+r}\right)^n \tag{23}$$

$$RC_{BESS} = ARC_{BESS} \times N_{BESS} \times \sum_{n=0}^{\left[\frac{y}{y_{BESS}}\right]-1} \frac{1}{(1+r)^{n \times y_{BESS}}} \tag{24}$$

In the above equations, AIC_{WT}, AIC_{PV} and AIC_{BESS} are the IC of each WT, PV panel and battery respectively; AOM_{WT}, AOM_{PV} and AOM_{BESS} are the annual OMC of WTs, PV system and BESS respectively; ARC_{BESS} represents the cost of each battery replacement; y_{BESS} is the lifetime of BESS.

The annual cost of exchanging energy with national power grid is given by Eq. (25).

$$C_{gird} = \sum_{t=1}^{T} \left\{ \left[\left[P_{Load}(t) + P_{ch}(t) \times \eta_1(t) - \frac{P_{dis}(t)}{\eta_{dis}} \times \mu_2(t) - P_{PV}(t) - P_{WT}(t) \right] \times P_t \right\} \times TC \tag{25}$$

where TC is an annualization coefficient. The value of C_{grid} is negative when the system sells electricity. On the contrary, the positive value of C_{grid} means the system is partly supplied by utility grid.

5.1.2. Pollution emissions

The application of FEVCS-WPE will have a positive impact on reducing global carbon emissions as the loads are mainly supplied by wind and PV power which are clean and pollution-free. Consequently, in FEVCS-WPE, the environmental pollution emissions mainly come from the part of the electricity purchased from the utility grid. Therefore, the second objective is to minimize the emissions of CO_2, SO_2 and NO_x, as shown in Eqs. (26) and (27).

$$E_{CO_2,SO_2,NO_x} = \sum_{t=1}^{T} \left(E_{CO_2}(t) + E_{SO_2}(t) + E_{NO_x}(t)\right) \tag{26}$$

$$E_{CO_2(t)} + E_{SO_2(t)} + E_{NOx(t)} = \begin{cases} 0 & P_{Grid}(t) \le 0 \\ P_{Grid}(t) \times \left(e_{CO_2} + e_{SO_2} + e_{NO_x}\right) & P_{Grid}(t) > 0 \end{cases} \tag{27}$$

where E_{CO_2,SO_2,NO_x} refers to the total emission of pollution. $E_{CO_2(t)}$, $E_{SO_2(t)}$ and $E_{NO_x(t)}$ represent the CO_2 emission, SO_2 emission and NO_x emission at time t respectively. e_{CO_2}, e_{SO_2} and e_{NO_x} are the emission factors of CO_2, SO_2 and NO_x respectively where $e_{CO_2} = 0.997$kg/kWh, $e_{SO_2} = 0.03$kg/kWh, $e_{NO_x} = 0.015$kg/kWh.

5.2. Constraints

The energy control center in FEVCS-WPE formulates the optimal operation strategy of the system according to the charging load requirements of EVs, so as to realize the power balance of the whole system. In the power scheduling process, the following constraints need to be satisfied.

(1) Equality constraint. It is the constraint of balance between supply and demand, which is the prerequisite for the stable and normal operation of FEVCS-WPE system. The amount of energy generation and consumption should be equal, given by Eq. (28).

$$P_{Load}(t) + P_{ch}(t) \times \eta_{ch} \times \mu_1(t) - \frac{P_{dis}(t)}{\eta_{dis}} \times \mu_2(t) - P_{PV}(t) - P_{WT}(t) = P_{Grid}(t) \tag{28}$$

where $P_{Grid}(t)$ is the power exchanged with utility grid.

(2) Inequality constraint. The inequality constraints are introduced in Section 4, including the charging/discharging power constraints and capacity constraints, etc.
(3) Integer constraint. The number of WTs N_{WT} and the number of batteries N_{BESS} must be positive integer variables.

5.3. Optimization algorithm

In order to obtain the optimal capacity configuration and scheduling strategy of FEVCS-WPE, this paper proposes a hybrid optimization algorithm based on MOPSO and TOPSIS. MOPSO is applied to solve the bi-objective optimization model and obtain the Pareto solutions, and TOPSIS is utilized to select the optimal one.

5.3.1. MOPSO algorithm

Particle swarm optimization (PSO) algorithm is an evolutionary algorithm based on birds' behavior and swarm intelligence. In PSO algorithm, each particle represents a possible solution and can be seen as an individual in a N-dimensional search space. Each particle has two properties: velocity and position. In the flight process, the velocity of each particle can be adjusted dynamically according to the personal and global optimal positions. The velocity represents how fast or slow it is moving, and the position represents its moving direction. These two properties are updated at each iteration according to Eqs. (29) and (30). In this paper, the population size in MOPSO is set as 50, and the maximum number of iterations is 200.

$$V_i(t) = wV_i(t-1) + c_1 r_1 (pbest_i(t-1) - p_i(t-1)) + c_2 r_2 (gbest_i(t-1) - p_i(t-1)) \tag{29}$$

$$p_i(t) = p_i(t-1) + V_i(t) \tag{30}$$

ω is the inertia weight. r_1, r_2 are random numbers in [0,1]. c_1,c_2 are learning factors and $c_1 = c_2 = 2$. $pbest_i$ and $gbest_i$are the personal and global optimum respectively.

It can be seen from the above equations that the inertial weight affects the flight velocity and direction of particles, thus affecting the convergence of the algorithm. Eberhart et al. pointed out that when the inertia weight is less than 0.4, PSO has a higher convergence speed but it is more likely to reach local optimum. When the inertia weight is greater than 0.9, the global search capability of the

algorithm is enhanced, but the number of iterations increases, and the convergence speed slows down. Therefore, in order to focus on global search at the beginning and accelerate the convergence after getting the uniformly distributed particle swarm, the value range of ω is limited in this study to decrease between [0.9, 0.4], as shown in Eq. (31).

$$w = w_{\max} - (w_{\max} - w_{\min}) \times \frac{t}{t_{\max}} \tag{31}$$

MOPSO algorithm was proposed by Carlos A. Coello Coello et al., in 2004 to apply PSO in multi-objective optimization problems and has been paid great attention because of its simple calculation process, convenient parameter setting and fast convergence, compared with NSGA-II, artificial neural network.

Compared to single-objective problems, multi-objective optimization is relatively complex in how to select global and personal optimal solutions. The MOPSO algorithm follows the following principles: randomly selecting one solution as the personal best position when the solutions are non-dominated; selecting a leader as the global optimum in the non-dominated solutions according to the crowding degree (CD) which is given by Eq. (32).

$$CD_i = \frac{|f_1(x_{i+1}) - f_1(x_{i-1})|}{f_1^{\max} - f_1^{\min}} + \frac{|f_2(x_{i+1}) - f_2(x_{i-1})|}{f_2^{\max} - f_2^{\min}} \tag{32}$$

The steps of the MOPSO algorithm are as follows:

(1) Initialize the position and velocity of the particles in the swarm and calculate the objective values of each particle.
(2) According to domination rule, obtain the Archive set which stores the non-dominated solutions.
(3) Calculate *pbest* and *gbest* according to the crowding degree shown in Eq. (32).
(4) Update the velocity, position and objective values of particles according to Eqs. (29) and (30)
(5) Update the Archive set.
(6) If the end condition is met, then stop the process. Otherwise, go to step (3) to continue the loop.

5.3.2. TOPSIS method

The basic process of TOPSIS is to normalize the decision matrix, select the positive and negative ideal solutions, compute the distances between each solution and ideal solutions and then determine the optimal solution based on close degree to positive ideal solution. This method has no strict limitation on data distribution and sample size, which is easily applied to multi-objective decision-making problems. In the proposed model, a number of Pareto solutions are obtained by MOPSO, and then the optimal solution will be determined by TOPSIS. The specific calculation steps of TOPSIS method are as follows.

(1) Build the decision matrix. Suppose there are n evaluation alternatives, which mean the Pareto solutions in this study, and m evaluation objectives. The decision matrix is given as below.

$$A = \begin{bmatrix} a_{11} & a_{12} & \cdots & a_{1m} \\ a_{21} & a_{22} & \cdots & a_{2m} \\ \vdots & \vdots & \ddots & \vdots \\ a_{n1} & a_{n2} & \cdots & a_{nm} \end{bmatrix}$$

(2) Normalize the decision matrix based on Eq. (33).

$$X_{ij} = (x_{ij})_{n*m} = a_{ij} \Big/ \left(\sum_{i=1}^{n} (a_{ij})^2 \right)^{1/2} \tag{33}$$

(3) Obtain the weighted decision matrix according to Eq. (34).

$$Y = \left(y_{ij}\right)_{n*m} = (w_j x_{ij})_{n*m} \tag{34}$$

where w_j is the weight of the jth objective.

(4) Determine the positive and negative ideal solutions based on Eqs. (35) and (36).

$$Y_0^+ = \left(\max_{1\le i\le n} y_{ij} \middle| \; j \in j^+, \min_{1\le i\le n} y_{ij} \middle| \; j \in j^- \right) = (y_1^+, y_2^+, \ldots y_m^+) \tag{35}$$

$$Y_0^- = \left(\min_{1\le i\le n} y_{ij} \middle| \; j \in j^+, \max_{1\le i\le n} y_{ij} \middle| \; j \in j^- \right) = (y_1^-, y_2^-, \cdots, y_m^-) \tag{36}$$

where Y_0^+ is the positive ideal solution (PIS) and Y_0^- is the negative ideal solution (NIS). j^+ is the benefit-type objective which means the bigger the better. j^- is the cost-type objective which means the smaller the better. The optimization objectives in the proposed model are both cost-type.

(5) Calculate the distance between samples and ideal solutions according to Eqs. (37) and (38). Euclidean distance is used to calculate the distance. The distance from the ith alternative to the PIS is D_i^+ and the distance to the NIS is expressed by D_i^-.

$$D_i^+ = \sqrt{\sum_{j=1}^{m} \omega_j \left(y_{ij} - y_{j^+}\right)^2} \; (i = 1, 2, \ldots n) \tag{37}$$

$$D_i^- = \sqrt{\sum_{j=1}^{m} \omega_j \left(y_{ij} - y_{j^-}\right)^2} \; (i = 1, 2, \ldots n) \tag{38}$$

(6) Calculate the close degree based on Eq. (39).

$$\delta_i = \frac{D_i^+}{D_i^+ + D_i^-}, (i = 1, 2, \ldots, n) \tag{39}$$

The solutions with higher δ_i are better. Therefore, the optimal solution can be determined based on the maximum δ_i.

The framework of the proposed algorithm is presented in Fig. 3.

6. Case study and discussion

An electric power company plans to build a FEVCS-WPE in Inner Mongolia, China. The output curves of a WT and a PV panel are obtained by collecting local wind speed, solar radiation and other data. Then, the load of EV charging piles at each moment is simulated. Finally, the proposed algorithm is used to investigate the optimal capacity of WT, PV system, BESS and the optimal power scheduling strategy. The proposed model is built in the MATLAB/Simulink R2017b environment and the environment is implemented in a computer with a processor Inter(R) Core(TM) i7-8550U CPU @ 1.8–2.0 GHz and 16G RAM.

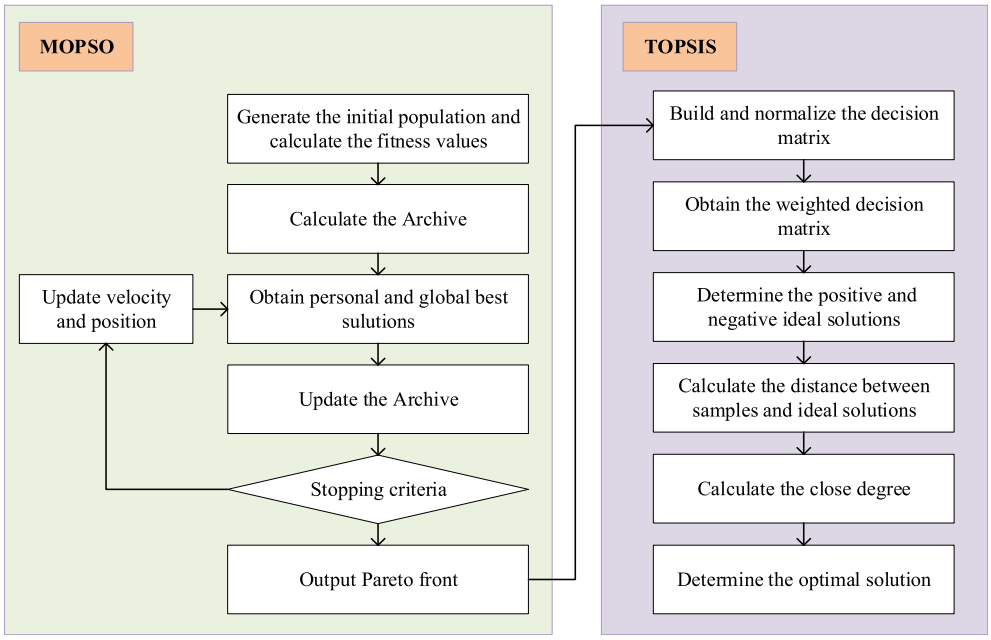

Fig. 3. The framework of the proposed algorithm.

6.1. Data collection

By collecting the wind speed and solar radiation from locally meteorological data, the output curves of a WT and a PV panel are calculated, as shown Fig. 4(a). The electricity exchange with utility grid is based on real-time electricity price, as shown in Fig. 4(b).

Other parameters required in this study are shown in Table 2.

6.2. EV demand simulation

In the proposed FEVCS-WPE, 10 fast charging piles are to be built, and their initial states are vacant. The rated power of each pile is 40 kW.

The service objects of the proposed FEVCS-WPE are mainly electric taxis and electric private cars, and therefore this study uses the data from an EV charging station in the neighborhood to simulate the load. By analyzing the statistical records of the local EV charging station for one month, the number of EV arriving at each hour is obtained and it is found that the initial SOC_S of EVs conforms to the normal distribution N $(0.4,0.1^2)$. On the basis of collected data, the charging load of EVs at each hour can be simulated by the model proposed in Section 3, as illustrated in Fig. 5.

6.3. Results and analysis

6.3.1. Result analysis

This study explains a model to optimize the design of the proposed FEVCS-WPE, including the capacity of components, power of BESS and energy exchanged with the national power grid. In this case, based on the collected data and EV load simulation result, the optimization design model is solved by MOPSO and 36 Pareto solutions are obtained, as shown in Fig. 6.

Since the Pareto solutions cannot dominate each other, in order to determine the optimal solution, TOPSIS method is applied to rank all 36 Pareto solutions. Each solution is considered as an evaluation alternative and each objective is a decision-making

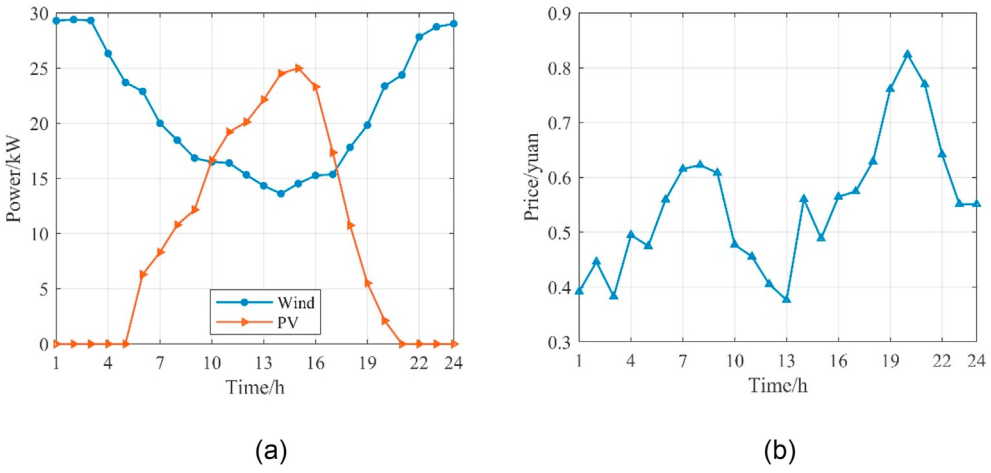

Fig. 4. The output curves of WT and PV.

Table 2
Parameters of system components.

Component	Parameter	Value	Unit
WT	Rated power	30	kW
	Cut-in speed	2.1	m/s
	Cut-out speed	20	m/s
	Rated speed	9	m/s
	Height of turbine hub	20	m
	Lifetime	25	Year
	IC	400000	Yuan/unit
	RC	300000	Yuan/unit
PV	Rated power	25	kW
	IC	250000	Yuan/unit
	OMC	700	Yuan/year
	Lifetime	25	year
	η_{PV}	85	%
	PV temperature coefficient	0.0045	–
	Cell reference temperature	25	$^{\circ}C$
	NOCT	55	$^{\circ}C$
BESS	Rated capacity	25	kWh
	IC	38000	Yuan/unit
	RC	35000	Yuan/unit
	OMC	700	Yuan/year
	DOD	20	%
	Self-discharge rate	0.002	
	Lifetime	20	Year
Other parameters	Interest rate	6	%

criterion. Suppose the weight of each objective is 0.5, the best solution is selected, as shown in Fig. 6.

In the optimal solution, the numbers of WTs, PV panels and batteries are respectively 11, 11.23, and 30. Therefore, the optimal capacity configuration of FEVCS-WPE is 330 kW, 280.75 kW and 750 kWh for WT, PV and BESS. Under this configuration, the objective values are $COE = 0.306 yuan/kWh$ and $E_{CO_2,SO_2,NO_x} = 472.38g$. The output of WTs and PV system is illustrated in Fig. 7(a), and the input/output values of BESS and utility grid per hour are presented in Fig. 7(b) and Table 3.

It can be seen that the BESS is in charging state in 9 h (2, 8, 10–12, 16, 18, 20–21), while it is in discharging state in other hours. At hour 1–2, 6–18, and 23–24, the system sells electricity to the utility grid to obtain incomes, and at other moments, the system buys electricity to replenish energy. According to the real-time electricity price, the cost of electricity exchanged with the utility grid in one day can be calculated as −368.04yuan, that is, the system can gain 368.04yuan from the utility grid, which can effectively reduce the COE by 0.049yuan/kWh.

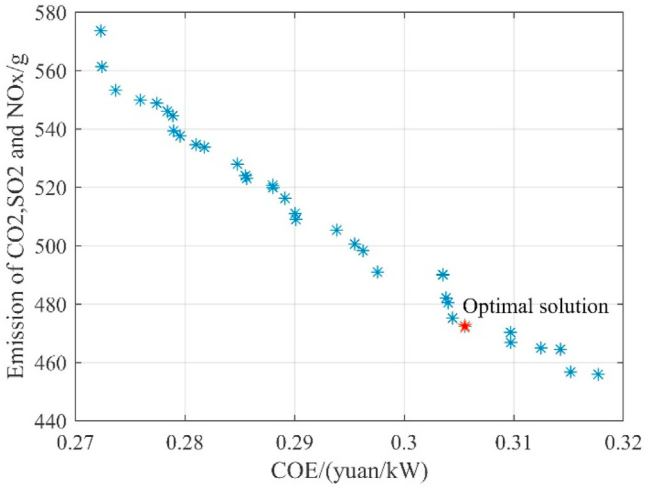

Fig. 6. The optimization result.

6.3.2. Scenario analysis

In order to fully reflect the influence of new energy supply and DR on the optimization result, the following three scenarios are analyzed.

(1) Scenario 1.

In this scenario, the fast EV charging station is supplied only by the utility grid. At this point, the cost of the charging station is only the power purchase cost from the utility grid, and the environmental pollution emission is directly related to the power exchange amount with the grid. In this scenario, the decision variables are the power exchanged with utility grid at each time interval.

In this scenario, the numbers of WTs, PV panels and batteries are 0, the COE is 0.559yuan/kWh and the pollution emission is 7710.8 g. Compared with the results of the proposed model, it is found that the COE in Scenario 1 increases by 0.253yuan/kWh and the pollution emission rises by 1532.33%. It is obvious that the application of wind and PV power can not only lower the COE, but also significantly reduce emissions of polluting gases.

(2) Scenario 2.

In this scenario, FEVCS-WPE is isolated from the utility grid and only supplied by renewable energies and BESS, which means it

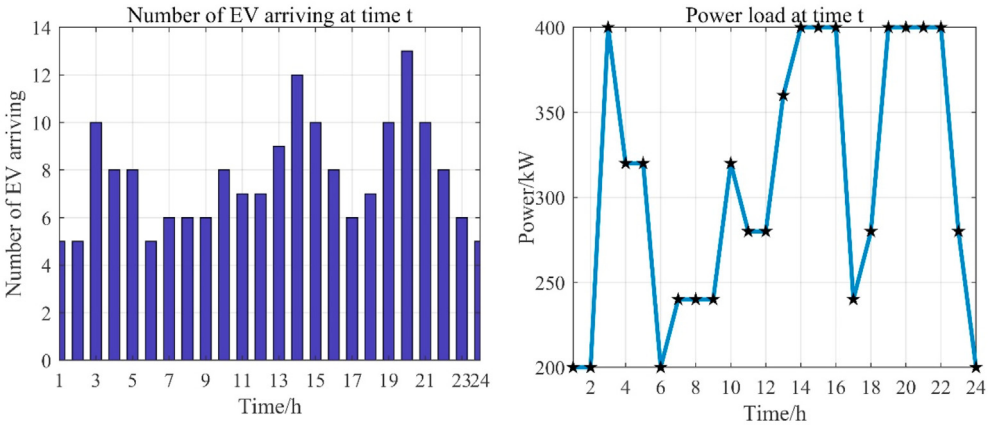

Fig. 5. The number of EVs and the power load.

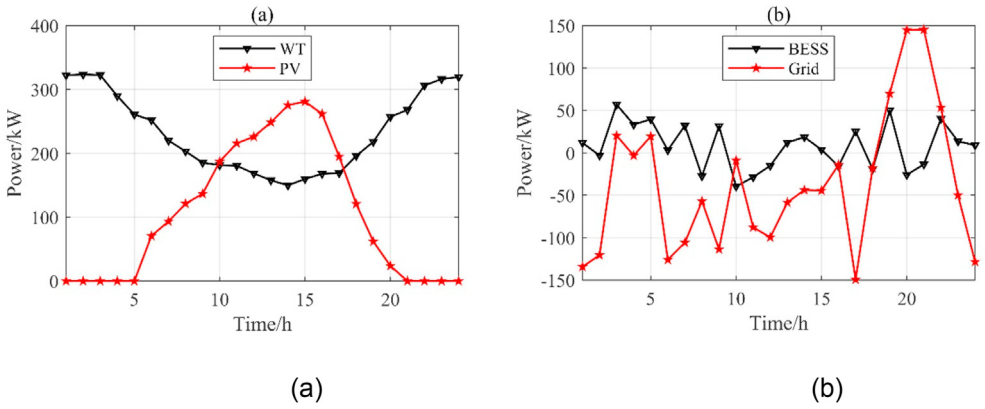

Fig. 7. The power of WT, PV, BESS and utility grid.

Table 3
The output power of WT, PV, BESS and utility grid.

t	Wind	PV	BESS	Grid	t	Wind	PV	BESS	Grid
1	322.34	0.00	11.91	−134.24	13	149.78	275.35	12.18	−58.53
2	323.44	0.00	−3.01	−120.42	14	159.87	280.81	18.68	−43.81
3	322.56	0.00	56.97	20.47	15	167.93	261.90	3.75	−44.43
4	289.70	0.00	33.45	−3.15	16	169.03	194.92	−15.72	−14.12
5	260.81	0.00	39.66	19.53	17	196.06	120.75	25.36	−149.31
6	251.94	70.80	3.20	−125.93	18	218.13	62.00	−19.14	−17.66
7	220.07	93.42	32.17	−105.66	19	257.14	23.85	50.12	69.74
8	203.17	121.20	−27.44	−56.93	20	268.22	0.00	−25.91	144.92
9	185.31	136.59	31.68	−113.58	21	306.24	0.00	−13.49	145.27
10	181.43	186.98	−39.58	−8.83	22	316.25	0.00	40.35	53.41
11	180.47	215.78	−28.62	−87.63	23	319.33	0.00	13.65	−49.90
12	168.59	226.04	−15.15	−99.48	24	149.78	275.35	8.99	−128.32

becomes an off-grid system. Since the charging station is completely cut off from the utility grid, the pollution emissions are zero. In this scenario, the decision variables are the number of WTs, PV panels and batteries, the charging/discharging power of BESS at each time interval.

According to the proposed optimization model, the optimal numbers of WTs, PV panels and batteries are 11, 9 and 22 respectively, and the COE is 0.317yuan/kWh. Compared with Scenario 1, the COE of this scenario is reduced by 0.242yuan/kWh (43.29%), and the environmental benefit of Scenario 2 is also much higher than scenario 1. Besides, compared with the base scenario, the COE in scenario 2 increases by 0.011yuan/kWh (3.59%). It can be seen that scenario 2 completely relies on the energy supply of new energy power generation, which protects the environment significantly. But because of being isolated from the utility grid, the system cannot obtain stable energy support, which leads to the lower flexibility and higher risks.

(3) Scenario 3.

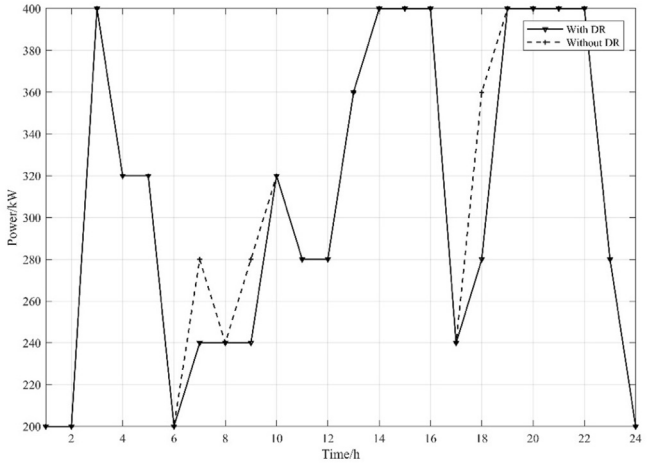

Fig. 8. The demand load with and without DR.

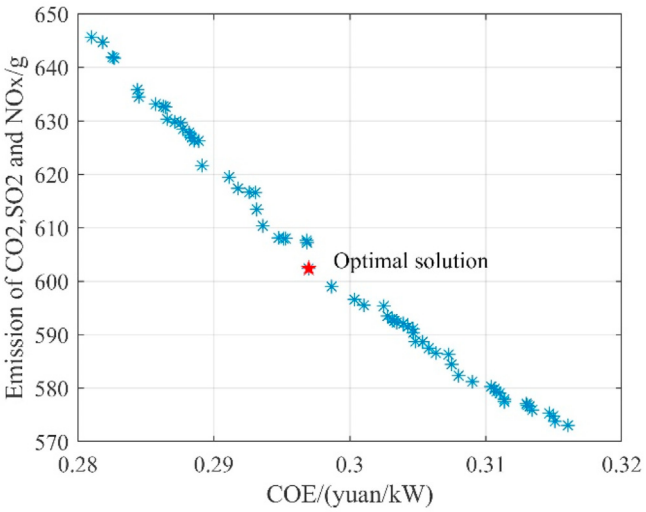

Fig. 9. The optimization result of scenario 3.

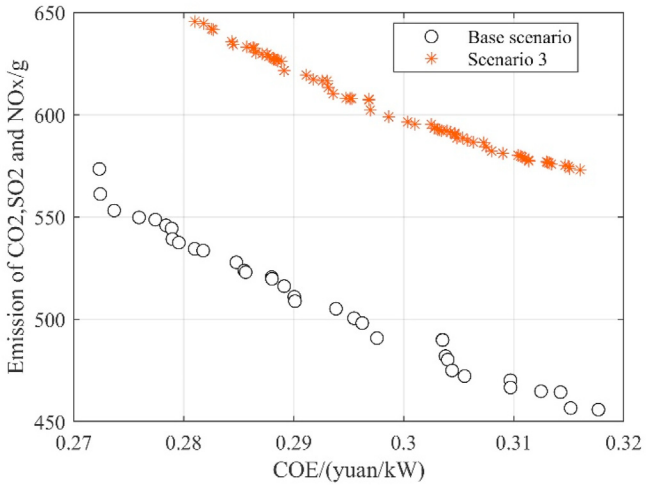

Fig. 10. The result comparison between base scenario and scenario 3.

In this scenario, the DR is not applied, which means the EV owners do not respond to the TOU electricity price. In this scenario, the decision variables are the number of WTs, PV panels and batteries, the charging/discharging power of BESS, and the power exchanged with utility grid at each time interval. The load of EVs without DR is shown in Fig. 8.

It can be seen that, the load at time 7, 9, and 18 is higher than the base scenario and the total load of this scenario increases slightly by 2.2%. Using the optimization method proposed in this paper, 65 Pareto solutions are obtained. The solution with the best economic objective is $N_{WT} = 11$, $N_{PV} = 12.72$, $N_{BESS} = 13$, with objective values COE = 0.281yuan/kWh and $E_{CO_2,SO_2,NO_x} = 645.652$ g while the solution with minimum pollution is $N_{WT} = 11$, $N_{PV} = 12.76$, $N_{BESS} = 32$ with the objective values COE = 0.316yuan/kWh and $E_{CO_2,SO_2,NO_x} = 573.07$ g. Then TOPSIS method is applied to select a compromised solution, which is $N_{WT} = 11$, $N_{PV} = 12.73$, $N_{BESS} = 24$ with COE = 0.297yuan/kWh and $E_{CO_2,SO_2,NO_x} = 602.413$ g. The optimization result of this scenario is presented in Fig. 9.

The base scenario and this scenario obtain 36 and 65 Pareto solutions respectively. The Pareto fronts are shown in Fig. 10. It is obvious that the results in base scenario are better than this scenario, which represents that DR can not only improve the flexibility of the system, but also effectively reduce the COE and improve environmental benefits.

6.3.3. Sensitivity analysis

The weight of the objectives reflects the preference of investors when they make decisions. When the COE objective function has a high weight, it means that investors are more inclined to obtain benefits from the system; otherwise, it means investors are more in pursuit of environmental benefits. Since decision-makers are subjective and flexible in determining weights, the system configuration and objective function values under the influence of different weight distribution are discussed, as shown in Fig. 11 and Table 4.

It can be seen that no matter how the weight distribution changes, the number of WTs is always fixed, remaining 11. The number of PV grows, and the number of batteries decreases with the increase of the weight of objective 1. Meanwhile, the change in weights directly reflects the change in the value of the objective functions. As shown in Fig. 11, as w_1 increases gradually, the value of COE decreases, while the pollution gas emissions become larger.

6.3.4. Comparative analysis

The literature review has mentioned that GA, SA and PSO are

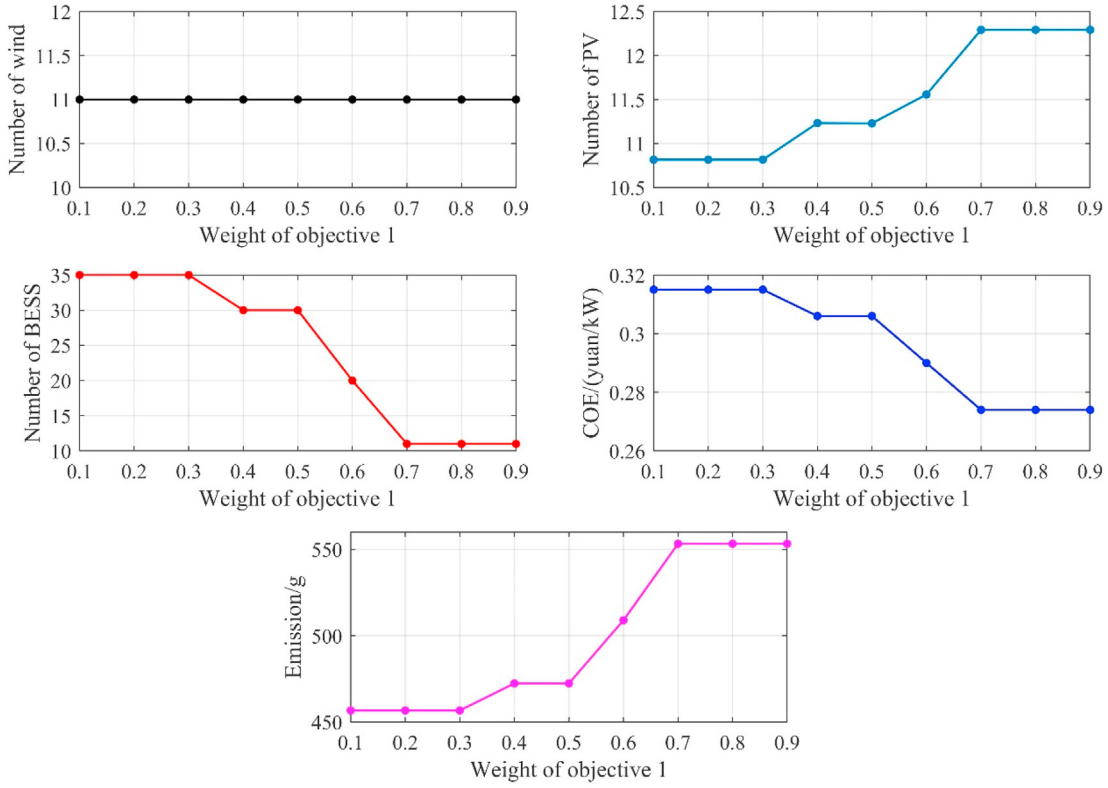

Fig. 11. The result of sensitivity analysis.

Table 4
The sensitivity analysis result.

w_1	w_2	WT	PV	BESS	COE	Pollution emissions
0.1	0.9	11	10.817	35	0.315	456.706
0.2	0.8	11	10.817	35	0.315	456.706
0.3	0.7	11	10.817	35	0.315	456.706
0.4	0.6	11	11.233	30	0.306	472.382
0.5	0.5	11	11.230	30	0.306	472.380
0.6	0.4	11	11.558	20	0.290	508.982
0.7	0.3	11	12.293	11	0.274	553.272
0.8	0.2	11	12.293	11	0.274	553.272
0.9	0.1	11	12.293	11	0.274	553.272

Table 5
The comparative analysis result.

	The proposed method	SA	GA
the number of WTs	11	11	11
the number of PV panels	11.23	11.76	11.43
the number of batteries	30	17	25
COE (yuan/kWh)	0.306	0.286	0.297
Emission (g)	472.38	523.94	480.66
Computing time (s)	13.04	267.44	325.63

widely used intelligent algorithms among all MOEA algorithms. Therefore, in order to prove the effectiveness of MOPSO algorithm, MOPSO was compared with GA and SA in this paper. Since the solutions obtained by the three methods are all non-dominated solutions, TOPSIS method is also used to select the optimal solution from the Pareto front for comparative analysis, as shown in Table 5.

It can be seen from the above table that the calculation speed of the proposed algorithm is 13.04s, which is significantly better than SA's 267.44s and GA's 325.63s. As the optimal solutions obtained by MOPSO-TOPSIS, SA-TOPSIS and GA-TOPSIS are all non-dominated, they cannot be directly compared. So the Pareto fronts obtained by MOPSO, SA and GA are compared and analyzed to rank the methods, as shown in Fig. 12.

In order to compare and analyze the Pareto solutions of these three methods, two comparison indexes are introduced in the paper (Xu et al., 2018) for further analysis. (1) The diversity of solutions(D), used to measure Pareto solution diversity, is a benefit indicator which means the greater the better. (2) Spacing metric(S), used to measure the uniformity of distribution of Pareto solutions, is a cost metric which means the less the better. The expression of these two indexes are presented as Eqs. 40 and 41.

Table 6
The comparison indexes of three methods.

	D	S
MOPSO	117.64	2.30
SA	75.73	3.60
GA	117.10	3.62

$$D = \sum_{k=1}^{2} \max\{|f_k(x_i) - f_k(x_j)|\} \tag{40}$$

$$S = \sqrt{\frac{1}{n-1}\sum_{i=1}^{n}(\overline{d} - d_i)^2} \tag{41}$$

where $d_i = \min\{|f_1(x_i) - f_1(x_j)| + |f_2(x_i) - f_2(x_j)|\}$.

As can be seen from Table 6, the MOPSO method has the highest D and the smallest S, indicating that this method is more suitable for the model constructed in this paper. In summary, compared with SA and GA, MOPSO not only has the fastest computing speed, but also can produce high-quality and satisfying Pareto solutions, enabling decision makers to make more precise investment decisions.

7. Conclusions and future work

Conclusively, it is significant for the development of clean energy to research on the capacity configuration and energy management of FEVCS-WPE. However, there are relatively few studies on this topic at present. Therefore, this paper proposed an optimization framework for capacity allocation and energy management of FEVCS-WPE. First, the EV power load was simulated dynamically based on a price-based DR model. Then, a bi-objective optimization model was built with the objectives of economic and environmental costs and solved by the MOPSO-TOPSIS method. Finally, the proposed framework was applied to a FEVCS-WPE in Inner Mongolia, China.

The main conclusions are remarked as follows.

(1) A simulation model of EV charging considering DR was proposed, in which the charging expectations of EVs were adjusted according the TOU electricity price. The EV charging process in a certain period was simulated and the load of the EV station was calculated.

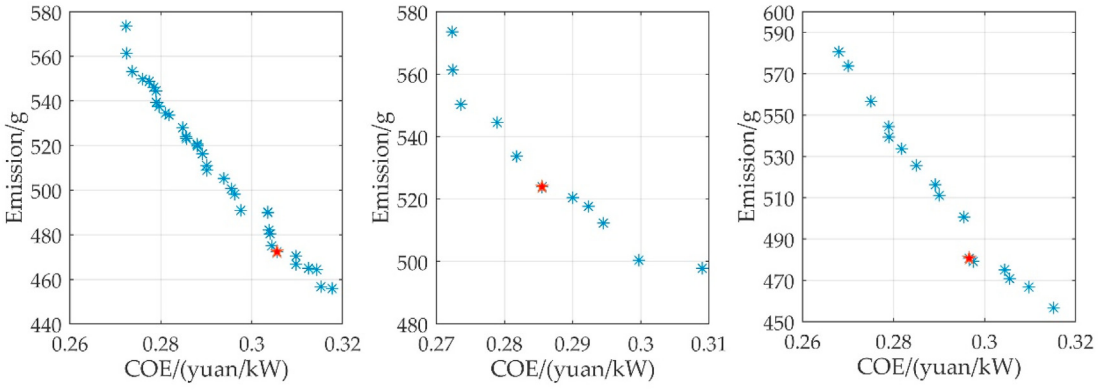

Fig. 12. The Pareto fronts of MOPSO, SA and GA.

(2) A bi-objective optimization design model for FEVCS-WPE were proposed to size WTs, PV system and BESS and determine optimal power scheduling strategy. To solve this model, a hybrid optimization algorithm was applied, in which MOPSO obtained Pareto front and TOPSIS selected the final optimal solution.
(3) A FEVCS-WPE is to be built in Inner Mongolia, China and the result indicates that the optimal capacity of WT, PV and batteries are 330 kW, 280.75 kW and 750 kWh with $COE = 0.306 yuan/kWh$ and $E_{CO_2,SO_2,NO_x} = 472.38g$.
(4) The scenario analysis concludes that the renewable energy supplies, the connection with utility grid and DR can help improve the performance on optimization objectives. In addition, a sensitivity analysis of objective weights was also performed, and it is concluded that with the increase of the COE objective, the number of WTs remains the same, the number of PV panels and batteries grows and decreases respectively.
(5) To demonstrate the effectiveness and superiority of the proposed framework, MOPSO was compared with SA and GA. The result shows that MOPSO had a running time of 13.04s, which was significantly better than SA's 267.44s and GA's 325.63s. Moreover, MOPSO had the highest diversity and the smallest spacing metric, which means the quality of the Pareto front was also better than the other two methods.

This paper sets the operating cycle of FEVCS-WPE as 1 day, that is, assuming that the operating state of each day remains consistent. In the future work, we will try to change the operating cycle of the system into week, month or year. In addition, the MOPSO, SA and GA have the same disadvantage that it is easy to fall into local optimum. Although this paper improved MOPSO by using the variable weight, there are still shortcomings. Therefore, in the future work, we will consider combining MOPSO method with other searching algorithms, such as harmony search and cuckoo search, to improve the accuracy of the results of the study.

CRediT authorship contribution statement

Baojun Sun: Conceptualization, Methodology, Software, Formal analysis, Writing - original draft, Writing - review & editing, Writing, Visualization.

Declaration of competing interest

The authors declare that they have no known competing financial interests or personal relationships that could have appeared to influence the work reported in this paper.

Acknowledgements

The author would appreciate the support of National Natural Science Foundation of China (71961022) and the help of the editor and reviewers.

Nomenclature

List of symbols

A	the decision matrix
ARC_{BESS}	the cost of each battery replacement
c_1	c_2 learning factors
C_{grid}	the annual cost of exchanging energy with utility grid
C_k	the cost of the kth component
D	the diversity of solutions
D_i^+	the distance from the ith alternative to the PIS
E	the battery capacity
$E_{BESS}(t)$	the electricity in BESS at time t
$E_{BESSmax}$	the maximum electricity allowed to be stored in BESS
e_{CO_2}	the emission factors of CO_2
$E_{CO_2}(t)$	the CO_2 emission at time t
E_{CO_2,SO_2,NO_x}	the total emission of pollution
$gbest_i$	the global optimum
$G_t(t)$	the solar radiation
h	the wind turbine height
h_{ref}	the wind tower height
j^+	the benefit-type objective
j^-	the cost-type objective
N_k	the number of the kth component
P	the charging power
$pbest_i$	the personal optimum
P_{BESS}	the rated power of BESS
$P_{ch}(t)$	the charging power at time t
$P_{dis}(t)$	the discharging power at time t
$P_{Grid}(t)$	the power exchanged with utility grid
$P_{load}(t)$	the EV charging load at time t
P_{PV-STC}	the rated power of PV panel
P_r	the output at rated speed
$P_{WT}(t)$	the output power at time t
r	discount rate
r_1, r_2	random numbers in [0,1]
S	spacing metric
SOC_E	the expected SOC
SOC_S	the start SOC
T_{amb}	the ambient temperature
T_C	the cell temperature
TC	an annualization coefficient
T_{cev}	charging duration
T_{C-STC}	the cell reference temperature
v_{cut-in}	cut-in speed
$v_{cut-out}$	cut-out speed
v_r	rated speed
v_{ref}	the wind speed at the wind tower
$v(t)$	the actual wind speed at time t
y	the system lifetime
Y_0^+	the positive ideal solution
Y_0^-	the negative ideal solution

Abbreviations

AC	alternating current
ANEC	augmented non-dominated constraint Method
BESS	battery energy storage system
CD	crowding degree
COE	cost of electricity
CRF	the capital recovery factor
DC	direct current
DOD	allowable depth of discharge
DR	demand response
EPoPA	extended power-pinch analysis
ESS	energy storage system
EV	electric vehicle
FEVCS-WPE	fast EV charging stations with wind, PV power and energy storage system
GA	genetic algorithm
IC	investment cost
LCC	life cycle cost
LPSP	loss of power supply probability
MADM	multi-attribute decision-making
MC	Monte Carlo
MOEA	multi-objective evolutionary algorithm

MOPSO	multi-objective particle swarm optimization
NIS	the negative ideal solution
NOCT	normal operation cell temperature
NPC	net present cost
NWCMO	weighted constrained multi-objective optimization
OM	operation and maintenance cost
PIS	the positive ideal solution
PV	photovoltaic
RC	replacement cost
SA	simulated annealing
SOC	state-of-charge
TOPSIS	Technique for Order Preference by Similarity to Ideal Solution
TOU	time-of-use
WT	wind turbines

Greek letters

ω	the inertia weight
η	the charging efficiency
η_{PV}	the generation efficiency
β_T	the temperature coefficient
σ	self-discharge rate
$\mu_1(t)$	charging state of BESS
$\mu_2(t)$	discharging state of BESS
δ_i	the close degree

References

Acuna, L.G., Padilla, R.V., Mercado, A.S., 2017. Measuring reliability of hybrid photovoltaic-wind energy systems: a new indicator. Renew. Energy 106, 68–77. https://doi.org/10.1016/j.renene.2016.12.089.

Amrollahi, M.H., Bathaee, S.M.T., 2017. Techno-economic optimization of hybrid photovoltaic/wind generation together with energy storage system in a stand-alone micro-grid subjected to demand response. Appl. Energy 202, 66–77. https://doi.org/10.1016/j.apenergy.2017.05.116.

Bae, S., Kwasinski, A., 2012. Spatial and temporal model of electric vehicle charging demand. IEEE Transactions on Smart Grid 3, 394–403. https://doi.org/10.1109/TSG.2011.2159278.

Baharin, N., Abdullah, T.A.R.T., 2013. Challenges of PHEV Penetration to the Residential Network in Malaysia. Procedia Technology.

Bukar, A.L., Tan, C.W., 2019. A review on stand-alone photovoltaic-wind energy system with fuel cell: system optimization and energy management strategy. J. Clean. Prod. 221, 73–88. https://doi.org/10.1016/j.jclepro.2019.02.228.

Chang, M., Bae, S., Yoon, G., Park, S., Choy, Y., 2019. Impact of electric vehicle charging demand on a jeju island radial distribution network. 2019. In: IEEE Power & Energy Society Innovative Smart Grid Technologies Conference (ISGT) 5.

Dai, Q., Liu, J., Wei, Q., 2019. Optimal photovoltaic/battery energy storage/electric vehicle charging station design based on multi-agent particle swarm optimization algorithm. Sustainability 11, 1973. https://doi.org/10.3390/su11071973.

Das, M., Singh, M.A.K., Biswas, A., 2019. Techno-economic optimization of an off-grid hybrid renewable energy system using metaheuristic optimization approaches - case of a radio transmitter station in India. Energy Convers. Manag. 185, 339–352. https://doi.org/10.1016/j.enconman.2019.01.107.

Das, R., Wang, Y., Putrus, G., Kotter, R., Marzband, M., Herteleer, B., Warmerdam, J., 2020. Multi-objective techno-economic-environmental optimisation of electric vehicle for energy services. Appl. Energy 257, 113965. https://doi.org/10.1016/j.apenergy.2019.113965.

Dominguez-Navarro, J.A., Dufo-Lopez, R., Yusta-Loyo, J.M., Artal-Sevil, J.S., Bernal-Agustin, J.L., 2019. Design of an electric vehicle fast-charging station with integration of renewable energy and storage systems. Int. J. Electr. Power Energy Syst. 105, 46–58. https://doi.org/10.1016/j.ijepes.2018.08.001.

Ekren, O., Ekren, B.Y., 2010. Size optimization of a PV/wind hybrid energy conversion system with battery storage using simulated annealing. Appl. Energy 87, 592–598. https://doi.org/10.1016/j.apenergy.2009.05.022.

Eriksson, E.L.V., Gray, E.M., 2019. Optimization of renewable hybrid energy systems - a multi-objective approach. Renew. Energy 133, 971–999. https://doi.org/10.1016/j.renene.2018.10.053.

Esfandyari, A., Norton, B., Conlon, M., McCormack, S.J., 2019. Performance of a campus photovoltaic electric vehicle charging station in a temperate climate. Sol. Energy 177, 762–771. https://doi.org/10.1016/j.solener.2018.12.005.

Esmaeili, S., Anvari-Moghaddam, A., Jadid, S., 2019. Optimal operation scheduling of a microgrid incorporating battery swapping stations. IEEE Trans. Power Syst. 34, 5063–5072. https://doi.org/10.1109/TPWRS.2019.2923027.

Fathabadi, H., 2017. Novel wind powered electric vehicle charging station with vehicle-to-grid (V2G) connection capability. Energy Convers. Manag. 136, 229–239. https://doi.org/10.1016/j.enconman.2016.12.045.

Fazlalipour, P., Ehsan, M., Mohammadi-Ivatloo, B., 2018. Optimal participation of low voltage renewable micro-grids in energy and spinning reserve markets under price uncertainties. Int. J. Electr. Power Energy Syst. 102, 84–96. https://doi.org/10.1016/j.ijepes.2018.04.010.

Gomez-Gonzalez, M., Hernandez, J.C., Vera, D., Jurado, F., 2020. Optimal sizing and power schedule in PV household-prosumers for improving PV self-consumption and providing frequency containment reserve. Energy 191, 116554. https://doi.org/10.1016/j.energy.2019.116554.

Hafez, O., Bhattacharya, K., 2020. Optimal design of electric vehicle charging stations considering various energy resources. Renew. Energy 147. https://doi.org/10.1016/j.renene.2019.08.113, 2527–2527.

Hakimi, S.M., Moghaddas-Tafreshi, S.M., 2009. Optimal sizing of a stand-alone hybrid power system via particle swarm optimization for Kahnouj area in south-east of Iran. Renew. Energy 34, 1855–1862. https://doi.org/10.1016/j.renene.2008.11.022.

Hernández, J.C., Sanchez-Sutil, F., Muñoz-Rodríguez, F.J., Baier, C.R., 2020. Optimal sizing and management strategy for PV household-prosumers with self-consumption/sufficiency enhancement and provision of frequency containment reserve. Appl. Energy 277, 1–22.

Javed, M.S., Song, A., Ma, T., 2019. Techno-economic assessment of a stand-alone hybrid solar-wind-battery system for a remote island using genetic algorithm. Energy 176, 704–717. https://doi.org/10.1016/j.energy.2019.03.131.

Kerdphol, T., Fuji, K., Mitani, Y., Watanabe, M., Qudaih, Y., 2016. Optimization of a battery energy storage system using particle swarm optimization for stand-alone microgrids. Int. J. Electr. Power Energy Syst. 81, 32–39. https://doi.org/10.1016/j.ijepes.2016.02.006.

Lee, T.-K., Bareket, Z., Gordon, T., Filipi, Z.S., 2012. Stochastic modeling for studies of real-world PHEV usage: driving schedule and daily temporal distributions. IEEE Trans. Veh. Technol. 61, 1493–1502. https://doi.org/10.1109/TVT.2011.2181191.

Li, M., Lenzen, M., Keck, F., McBain, B., Rey-Lescure, O., Li, B., Jiang, C., 2019. GIS-based probabilistic modeling of BEV charging load for Australia. Ieee Transactions on Smart Grid 10, 3525–3534. https://doi.org/10.1109/TSG.2018.2829917.

Li, C., Jia, X., Zhou, Y., Li, X., 2020. A microgrids energy management model based on multi-agent system using adaptive weight and chaotic search particle swarm optimization considering demand response. J. Clean. Prod. 262, 121247. https://doi.org/10.1016/j.jclepro.2020.121247.

Liu, Z., Chen, Y., Zhuo, R., Jia, H., 2018. Energy storage capacity optimization for autonomy microgrid considering CHP and EV scheduling. Appl. Energy 210, 1113–1125. https://doi.org/10.1016/j.apenergy.2017.07.002.

Liu, L., Sun, L., Chen, Y., Ma, X., 2019. Optimizing fleet size and scheduling of feeder transit services considering the influence of bike-sharing systems. J. Clean. Prod. 236 https://doi.org/10.1016/j.jclepro.2019.07.025. UNSP 117550.

Ma, T., Yang, H., Lu, L., 2014. A feasibility study of a stand-alone hybrid solar-wind-battery system for a remote island. Appl. Energy 121, 149–158. https://doi.org/10.1016/j.apenergy.2014.01.090.

Mazzeo, D., Baglivo, C., Matera, N., Congedo, P.M., Oliveti, G., 2020a. A novel energy-economic-environmental multi-criteria decision-making in the optimization of a hybrid renewable system. Sustainable Cities and Society 52, 101780. https://doi.org/10.1016/j.scs.2019.101780.

Mazzeo, D., Matera, N., De Luca, P., Baglivo, C., Congedo, P.M., Oliveti, G., 2020b. Worldwide geographical mapping and optimization of stand-alone and grid-connected hybrid renewable system techno-economic performance across Koppen-Geiger climates. Appl. Energy 276, 115507. https://doi.org/10.1016/j.apenergy.2020.115507.

Mercier, P., Cherkaoui, R., Oudalov, A., 2009. Optimizing a battery energy storage system for frequency control application in an isolated power system. IEEE Trans. Power Syst. 24, 1469e77.

Moghaddam, A.A., Seifi, A., Niknam, T., Pahlavani, M.R.A., 2011. Multi-objective operation management of a renewable MG (micro-grid) with back-up micro-turbine/fuel cell/battery hybrid power source. Energy 36, 6490–6507. https://doi.org/10.1016/j.energy.2011.09.017.

Moghaddam, A.A., Seifi, A., Niknam, T., 2012. Multi-operation management of a typical micro-grids using Particle Swarm Optimization: a comparative study. Renew. Sustain. Energy Rev. 16, 1268–1281. https://doi.org/10.1016/j.rser.2011.10.002.

Montoya, O.D., Gil-Gonzalez, W., Hernandez, J.C., Giral-Ramirez, D.A., Medina-Quesada, A., 2020. A mixed-integer nonlinear programming model for optimal reconfiguration of DC distribution feeders. Energies 13, 4440. https://doi.org/10.3390/en13174440.

Naidu, K., Mokhlis, H., Bakar, A.H.A., 2014. Multiobjective optimization using weighted sum artificial bee colony algorithm for load frequency control. Int. J. Electr. Power Energy Syst. 55, 657–667. https://doi.org/10.1016/j.ijepes.2013.10.022.

Nguyen, T.A., Crow, M.L., Elmore, A.C., 2015. Optimal sizing of a vanadium redox battery system for microgrid systems. Ieee Transactions on Sustainable Energy 6, 729–737. https://doi.org/10.1109/TSTE.2015.2404780.

Nguyen, H.T., Safder, U., Nguyen, X.Q.N., Yoo, C., 2020. Multi-objective decision-making and optimal sizing of a hybrid renewable energy system to meet the dynamic energy demands of a wastewater treatment plant. Energy 191, 116570. https://doi.org/10.1016/j.energy.2019.116570.

Pan, Y., Qiu, X., Wu, J., Xiao, J., 2018. Analysis on charging behaviors of electric vehicles based on Markov decision processes. Electric Power Construction 39, 129–137.

Ramli, M.A.M., Bouchekara, H.R.E.H., Alghamdi, A.S., 2018. Optimal sizing of PV/wind/diesel hybrid microgrid system using multi-objective self-adaptive differential evolution algorithm. Renew. Energy 121, 400–411. https://doi.org/10.1016/j.renene.2018.01.058.

Ren, T., Li, X., Chang, C., Chang, Z., Wang, L., Dai, S., 2019. Multi-objective optimal analysis on the distributed energy system with solar driven metal oxide redox cycle based fuel production. J. Clean. Prod. 233, 765–781. https://doi.org/10.1016/j.jclepro.2019.06.028.

Sarshar, J., Moosapour, S.S., Joorabian, M., 2017. Multi-objective energy management of a micro-grid considering uncertainty in wind power forecasting. Energy 139, 680–693. https://doi.org/10.1016/j.energy.2017.07.138.

Shakerighadi, B., Anvari-Moghaddam, A., Ebrahimzadeh, E., Blaabjerg, F., Bak, C.L., 2018. A hierarchical game theoretical approach for energy management of electric vehicles and charging stations in smart grids. Ieee Access 6, 67223–67234. https://doi.org/10.1109/ACCESS.2018.2878903.

Shang, C., Srinivasan, D., Reindl, T., 2016. An improved particle swarm optimisation algorithm applied to battery sizing for stand-alone hybrid power systems. Int. J. Electr. Power Energy Syst. 74, 104–117. https://doi.org/10.1016/j.ijepes.2015.07.009.

Singh, G., Baredar, P., Singh, A., Kurup, D., 2017. Optimal sizing and location of PV, wind and battery storage for electrification to an island: a case study of Kavaratti, Lakshadweep. Journal of Energy Storage 12, 78–86. https://doi.org/10.1016/j.est.2017.04.003.

Sun, W., Wang, C., Zhang, C., 2017. Factor analysis and forecasting of CO2 emissions in Hebei, using extreme learning machine based on particle swarm optimization. J. Clean. Prod. 162, 1095–1101. https://doi.org/10.1016/j.jclepro.2017.06.016.

Tito, S.R., Lie, T.T., Anderson, T.N., 2016. Optimal sizing of a wind-photovoltaic-battery hybrid renewable energy system considering socio-demographic factors. Sol. Energy 136, 525–532. https://doi.org/10.1016/j.solener.2016.07.036.

Vermaak, H.J., Kusakana, K., 2014. Design of a photovoltaic-wind charging station for small electric Tuk-tuk in DRCongo. Renew. Energy 67, 40–45. https://doi.org/10.1016/j.renene.2013.11.019.

Wang, R., Li, G., Ming, M., Wu, G., Wang, L., 2017. An efficient multi-objective model and algorithm for sizing a stand-alone hybrid renewable energy system. Energy 141, 2288–2299. https://doi.org/10.1016/j.energy.2017.11.085.

Xu, F., Liu, J., Lin, S., Yuan, J., 2017. A VIKOR-based approach for assessing the service performance of electric vehicle sharing programs: a case study in Beijing. J. Clean. Prod. 148, 254–267. https://doi.org/10.1016/j.jclepro.2017.01.162.

Xu, F., Liu, J., Lin, S., Dai, Q., Li, C., 2018. A multi-objective optimization model of hybrid energy storage system for non-grid-connected wind power: a case study in China. Energy 163, 585–603. https://doi.org/10.1016/j.energy.2018.08.152.

Xu, X., Hu, W., Cao, D., Huang, Q., Chen, C., Chen, Z., 2020. Optimized sizing of a standalone PV-wind-hydropower station with pumped-storage installation hybrid energy system. Renew. Energy 147, 1418–1431. https://doi.org/10.1016/j.renene.2019.09.099.

Yang, H., Zhou, W., Lou, C., 2009. Optimal design and techno-economic analysis of a hybrid solar-wind power generation system. Appl. Energy 86, 163–169. https://doi.org/10.1016/j.apenergy.2008.03.008.

Yi, T., Zhang, C., Lin, T., Liu, J., 2020. Research on the spatial-temporal distribution of electric vehicle charging load demand: a case study in China. J. Clean. Prod. 242 https://doi.org/10.1016/j.jclepro.2019.118457. UNSP 118457.

Yousefi, H., Ghodusinejad, M.H., Noorollahi, Y., 2017. GA/AHP-based optimal design of a hybrid CCHP system considering economy, energy and emission. Energy Build. 138, 309–317. https://doi.org/10.1016/j.enbuild.2016.12.048.

Zhang, Y., Han, Q., 2017. Development of electric vehicles for China's power generation portfolio: a regional economic and environmental analysis. J. Clean. Prod. 162, 71–85. https://doi.org/10.1016/j.jclepro.2017.06.024.

Zhang, H., Hu, Z., Song, Y., Xu, Z., Jia, L., 2014. A prediction method for electric vehicle charging load considering spatial and temporal distribution. Autom. Electr. Power Syst. 38, 13–20.

Zhang, W., Chen, L., Huang, Y., Niu, L., Huang, M., Zhang, D., Shi, W., 2015. Application of M/G/k queuing model in queuing system of electric taxi charging station. Power Syst. Technol. 39, 724–729.

Zhang, W., Maleki, A., Rosen, M.A., Liu, J., 2019. Sizing a stand-alone solar-wind-hydrogen energy system using weather forecasting and a hybrid search optimization algorithm. Energy Convers. Manag. 180, 609–621. https://doi.org/10.1016/j.enconman.2018.08.102.

Zhang, B., Xu, L., Zhang, J., 2020. A multi-objective cellular genetic algorithm for energy-oriented balancing and sequencing problem of mixed-model assembly line. J. Clean. Prod. 244, 118845. https://doi.org/10.1016/j.jclepro.2019.118845.